Water Absorption and Disc Cracking in Urethane–Methacrylate Resins

CLIVE B. BUCKNALL,[1,*] XIANG CHENG ZHANG,[1] MICHAEL L. ORTON,[2] and GRAHAM V. JACKSON[2]

[1]Cranfield Institute of Technology, Bedford MK43 OAL and [2]ICI Chemicals & Polymers Ltd, The Heath, Runcorn, Cheshire WA7 4QD, United Kingdom

SYNOPSIS

Water absorption at 23 and 100°C has been studied in three materials based on a single type of urethane–methacrylate resin: the neat resin, a rubber-toughened blend containing 15 wt % of core-shell modifier, and a filled rubber-toughened resin containing 46 wt % silica plus 8 wt % core-shell modifier. In all six absorption experiments, water diffusion followed Fick's law. However, in neat resin at 100°C, the period of Fickian diffusion, during which the material appeared to reach saturation, was followed by an additional period of water uptake, which was accompanied by formation of internal disc cracks up to 1 mm in diameter. At both 23 and 100°C, fracture of water-saturated neat resin was defect dominated: cracks were initiated at inorganic impurities between 40 and 80 μm in diameter. The adverse effects of water are attributed to hydration and consequent swelling of these insoluble impurities. No internal cracking was detected in either the rubber-modified or hybrid resin, which have higher a K_{IC}s than the neat resin. © 1994 John Wiley & Sons, Inc.

INTRODUCTION

Disc cracking in thermosetting resins has been reported by Lee et al.,[1] who observed internal cracks in unsaturated polyester resin samples that had been immersed in water at 40–90°C for periods of several weeks. Both the positions of the crack nuclei, and the planes on which the disc cracks formed, appeared to be random. The authors attributed this cracking to hydrolysis of the resin to form water-soluble products, which forced internal surfaces apart by generating an osmotic pressure. In 1980, Fedors reported similar disc cracks in epoxy resin[2] and in rubber[3] containing deliberately added inclusions. In his experiments, the primary requirement for cracking was that inclusions were water soluble: again, osmotic pressure was identified as the cause.

The present paper describes another example of disc cracking following prolonged immersion of a thermosetting resin in water. In this case, cracking is associated with insoluble impurities, which are found at the origin of each crack. Failures of this type did not occur in rubber-modified grades of the same resin. The factors affecting diffusion and fracture, and the mechanisms responsible for initiating disc cracks, are discussed below.

EXPERIMENTAL

Materials

The resin used in this program was ICI's development grade Modar 8035, which in its uncured state is a solution of methacrylate-terminated urethane oligomer molecules in methyl methacrylate monomer. Curing is initiated through a peroxide, and leads to the formation of a cross-linked network containing both urethane and methacrylate segments. Impact-resistant grades were made by blending the uncured resin with Rohm and Haas Paraloid BTA 753, a particulate modifier in which a PMMA shell is grafted onto a cross-linked polybutadiene core. The elastomeric core in this type of particle has a diameter in the order of 0.1 μm. A mineral filler (cristobalite silica flour XPT6) was added to rubber-modified liquid Modar resin to form hybrid com-

* To whom correspondence should be addressed.

Journal of Applied Polymer Science, Vol. 52, 457–466 (1994)
 CCC 0021-8995/94/030457-10

posites. The filler has 50 wt % of particles below 10 μm, 25% below 4 μm, and a specific gravity of 2.33. The initiator system was a combination of 1% benzoyl peroxide (BPO), as 36% active paste, and 0.5% *N,N*-dimethylaniline (DMA) catalyst, quantities being based on the amount of resin in each polymerization.

In making rubber-toughened resins, the modifier was mixed into Modar 8035 resin, at a ratio of 15 : 85, and left to degas at 23°C under a reduced pressure of 600 mmHg before cure. Cured toughened Modar has a specific gravity of 1.17. The coupling agent A174, 3-(trimethoxysilyl)-propylmethacrylate, was added to the silica-filled systems at a concentration of 0.5% based on weight of filler. Mixing was carried out at 23°C using a 4-bladed Silverson internal mixer.

In this article, the three materials: neat Modar, rubber-modified, and rubber-modified/filled resins are termed *T00F00, T15F00,* and *T15F46,* where T15 indicates a concentration of 15 wt % modifier *in the polymer,* and F46 means an *overall* percentage of 46 wt % filler. Thus the hybrid material T15F46 contains 8.1 parts of modifier, 45.9 parts of Modar resin, and 46 parts of silica.

Moisture Measurement

The specimens used to measure rates of water uptake were squares about 10 × 10 mm, with a thickness of 0.7–1.0 mm. In order to provide a baseline for these absorption experiments, all specimens were preconditioned in a vacuum oven at 65°C for 4 days. A large batch of preconditioned specimens was placed in distilled water at either 100 or 23°C, and sets of three were withdrawn at intervals for determination of water content, using a Mitsubishi Moisture Meter CA-05. Saturation water contents were also measured independently by immersing preconditioned 4 × 8 × 35 mm blocks of all three materials in distilled water at 23°C for over a year, and weighing at intervals.

Tensile Tests

Fracture strength at 23°C was measured in uniaxial tension, using dumbbell-shaped specimens with a 40-mm gauge length, and 2.6 × 5.6 mm cross-section, at a cross-head speed 0.5 mm min^{-1}. Tensile specimens were immersed in distilled water at 100°C for up to 7 weeks, then dried for at least 5 days under full vacuum at 65°C before testing.

Fracture Toughness Tests

Fracture toughness was measured using single-edge notched bending (SENB) specimens, following the procedures laid down in the current European Protocol,[4] except that two fixed pins were used in place of the roller pins recommended in the Protocol. Tests were carried out at a cross-head speed of 0.5 mm/min.

Microscopy

An Olympus BH-2 optical microscope was used to observe internal disc cracks, and a Cambridge Stereoscan Model 250 MK3 scanning electron microscope, equipped with energy-dispersive X-ray analysis (EDAX) facilities, was used to determine the elemental composition of impurities located at crack nuclei.

RESULTS

For the case of Fickian diffusion into a wide, thin sheet, M_t, the mass of water absorbed in time t, is related to M_s, the mass absorbed at saturation, by[5]

$$\frac{M_t}{M_s} = 1 - \sum_{n=0}^{\infty} \frac{8}{(2n+1)^2\pi^2} e^{-D(2n+1)^2\pi^2 t/b^2} \quad (1)$$

where D is the diffusion coefficient and b is the thickness of the sheet, here taken as very small compared with the other two dimensions, so that diffusion is limited to the through-thickness direction.

For small values of t, Eq. (1) can be replaced by the following approximate expression:

$$\frac{M_t}{M_s} = 4\left(\frac{Dt}{b^2}\right)^{1/2} \times \left[\pi^{-1/2} + 2\sum_{n=0}^{\infty} (-1)^n \text{erfc}\left(\frac{nb}{2\sqrt{Dt}}\right)\right] \quad (2)$$

A further approximation can be made, involving only the leading term in Eq. (2) as follows:

$$\frac{M_t}{M_s} \approx 4\left(\frac{Dt}{\pi b^2}\right)^{1/2} \quad (3)$$

This can be used to obtain the diffusion coefficient D, with a systematic error of less than 1% when $M_t/M_s < 0.6$.

Experimental results on water absorption for the three Modar-based materials are presented in Figures 1 and 2, which show that M_t/M_s increases linearly with $t^{1/2}/b$ during the initial period of water absorption, as predicted by Eq. (3). Diffusion coefficients obtained from these curves are summarized in Table I. Saturated water concentrations M_s are given in the same table. With one exception, they are taken from long-term immersion tests. The exception is the neat resin at 100°C, in which the water uptake increases suddenly after the sample has apparently reached equilibrium, and for which M_s is therefore taken from the point of *apparent* equilibrium.

It can seen from the table that for each of the three materials, diffusion coefficients D are two orders of magnitude higher at 100 than at 23°C. Blending with the modifier has little effect on D, whereas addition of silica filler reduces it by 20–25%. Similar trends are seen in equilibrium water concentrations, but with a more marked reduction of 44% on adding filler.

Comparisons of experimental data with the predictions of Fick's law are shown in Figures 3 and 4. The solid lines, obtained using Eq. (1), relate the normalized water absorption M_t/M_s to the dimensionless time Dt/b^2. At 23°C, the results for the unmodified Modar resin fit Fick's law well. However, for the rubber-toughened resin and the hybrid composite there are deviations from Fickian behavior: rates of water uptake are a little higher than predicted during in the initial period, and substantially lower later. At 100°C, the data fit Fick's law better, except in the neat resin, where water absorption appears to approach equilibrium, but then suddenly rises, as noted earlier.

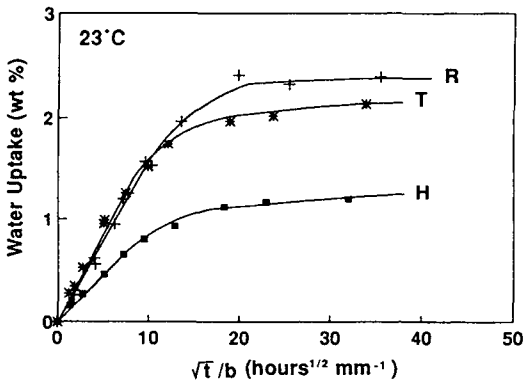

Figure 1 Fickian plot of water uptake at 23°C against (immersion time)$^{1/2}$ for (R) neat resin, (T) toughened resin T15F00, and (H) hybrid resin T15F46.

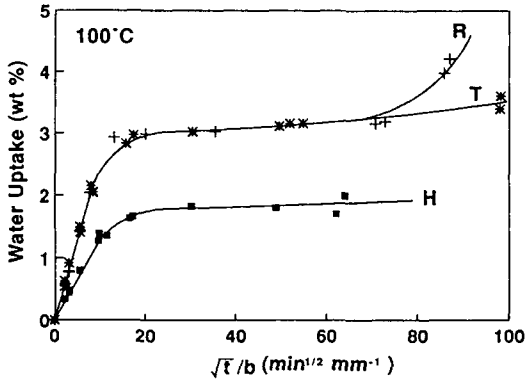

Figure 2 Fickian plot of water uptake at 100°C for same materials as Figure 1.

This anomalous water absorption behavior is accompanied by the appearance of visible internal disc cracks in the neat resin specimens. A typical example is shown in Figure 5. At its center is an irregularly shaped impurity about 30 μm across. Elemental analysis using EDAX reveals the presence of Na, Al, Si, S, Cl, Ca, and Cr, as shown in Figure 6. Similar inorganic impurities were found at the centers of all disc cracks examined. In addition, analyses of other inorganic impurities at crack centers have detected Fe, K, and Mg.[6] Disc cracking accounts for the unexpected increase in water absorption: there is no evidence of either disc cracking or anomalous water uptake in the rubber-toughened resin T15F00 or the hybrid resin T15F46.

In order to measure the amount of permanent damage resulting from water absorption, tensile specimens of neat Modar 8035 resin were immersed in distilled water at 100°C for periods between 0 and 46 days. These specimens were then dried under full vacuum at 65°C for about 7 days, cooled slowly to 23°C, and placed in a desiccator at 23°C prior to testing. The results are presented in Figure 7 and Table II: tensile strength σ_f is initially high, at ~ 80 MPa, but shows a marked fall between 11 and 26 days immersion, coinciding with the appearance of disc cracks. After 46 days immersion, σ_f is below 40 MPa. Even before visible disc cracks appear and tensile strength begins to fall, the effects of water treatment can be seen in the location of crack nuclei, which are summarized in Figure 8. Initially, half of the specimens fail from corners, and the other half from the surfaces of the bar, as expected in well-made specimens. However, after 4 days immersion, failures occur mainly from internal crack nuclei; and after 36 days, all failures are from internal defects. In all three types of initiation site, the origin of the crack defines the center of a circular arc, within

Table I Water Absorption Parameters

Materials	T00F00		T15F00		T15F46	
T (°C)	23	100	23	100	23	100
D ($\mu m^2\ s^{-1}$)	0.21	21.7	0.22	20.2	0.18	15.2
M_s (wt %)	2.5	3.2	2.5	3.2	1.4	1.8

which the fracture surface is mirror-like, and beyond which it is marked with parabolic steps.

Table III compares the results of fracture toughness tests on three types of bars: (1) "normal" specimens, which were equilibrated with the laboratory atmosphere at 23°C; (2) "dried" moisture-free resins; and (3) "wet" water-saturated specimens. The "wet" samples were immersed in water for 20 days at 100°C, cooled slowly, and kept under water until ready for testing. A considerable increase in K_{IC} was obtained after rubber modification, and a further increase was achieved by incorporation of filler. Moisture appears to have little influence on K_{IC} except in neat Modar, where it increases fracture resistance.

DISCUSSION

From Table I, it is clear that adding 15% of the core-shell modifier has little effect on either the diffusion behavior or the saturated water content of Modar resin. On the other hand, 46 wt % of silica (equivalent to 30 vol %) reduces D by 20–25% and M_s by 44%. In comparison with the values expected from the rule of mixtures, diffusion rates in the filled material are rather higher than expected, and saturation levels are substantially lower. The latter point is illustrated in Figure 9, which shows water uptake of the rubber-modified resin component of T15F00 and T15F46 as a function of $\sqrt{t}/b$. Assuming that water absorption by the silica is negligible, and allowing for the reduced polymer content of the filled polymer, M_s for T15F46 should be 1.75% at 23°C, and 2.20% at 100°C, whereas the measured values are 1.4% and 1.8%, only about 80% of those predicted.

A possible reason for the reduced water content at saturation in the hybrid resin is that regions of polymer immediately adjacent to the filler particles are in compression, owing to shrinkage of the resin during cure. The volumetric cure shrinkage of neat Modar 8035 is 11.3%,[6] but this figure will be reduced in the water-saturated filled resin by two factors: the presence of 15% nonshrinking core-shell modifier, and the increase in volume due to swelling with about 2 wt % of water. The net effect is to reduce the average volume shrinkage of the polymeric component of the water-saturated hybrid to about 8%, equivalent to a linear shrinkage of 2.6%. This figure

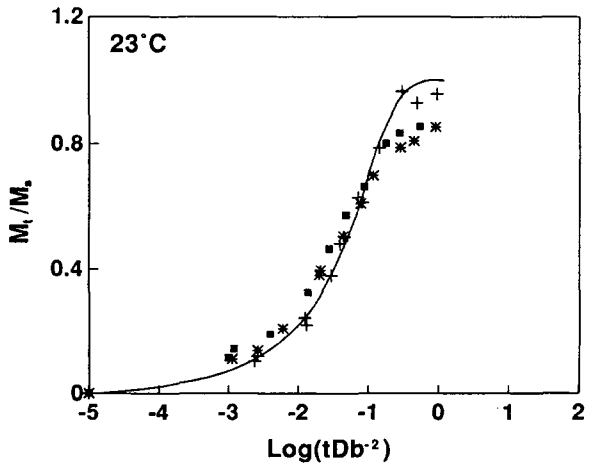

Figure 3 Relationship between normalized water absorption at 23°C and reduced time for (+) neat resin T00F00, (✳) toughened resin T15F46, and (■) hybrid resin T15F46. Solid line represents Eq. (1).

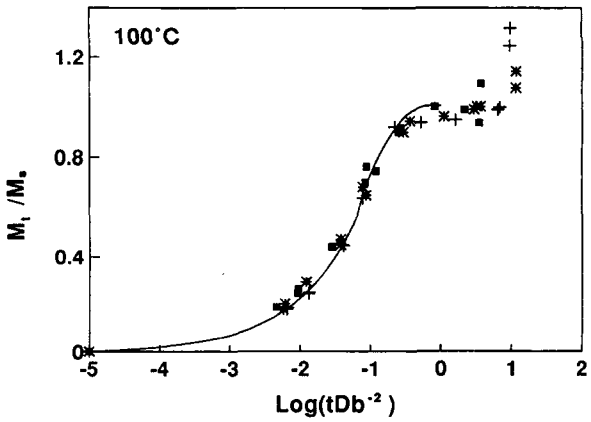

Figure 4 Relationship between normalized water absorption at 100°C and reduced time. Symbols as per Figure 3.

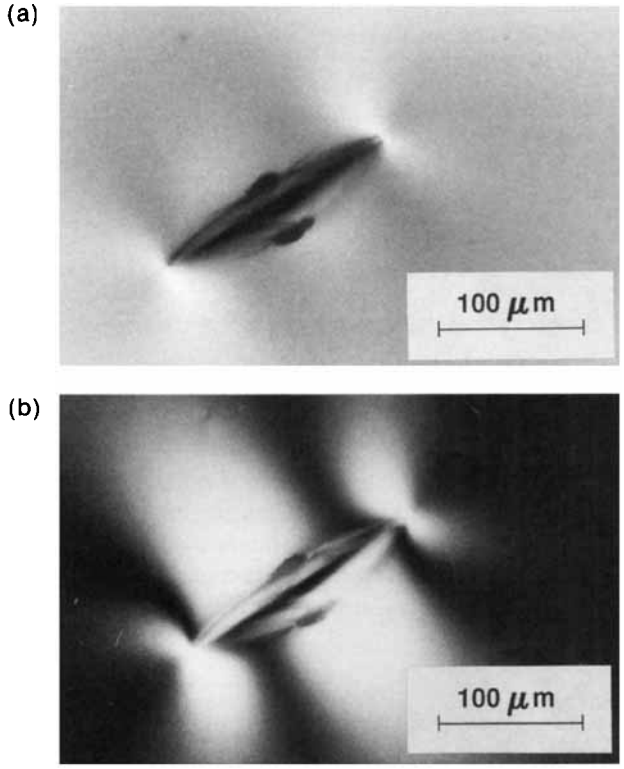

Figure 5 Optical micrograph of solid impurity with surrounding disc crack in neat resin (a) in plain light and (b) between crossed polars.

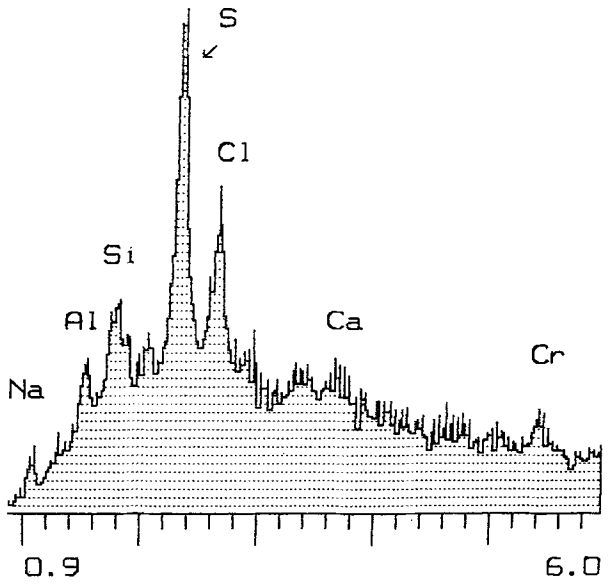

Figure 6 EDAX scan showing elemental composition of an impurity in the neat resin.

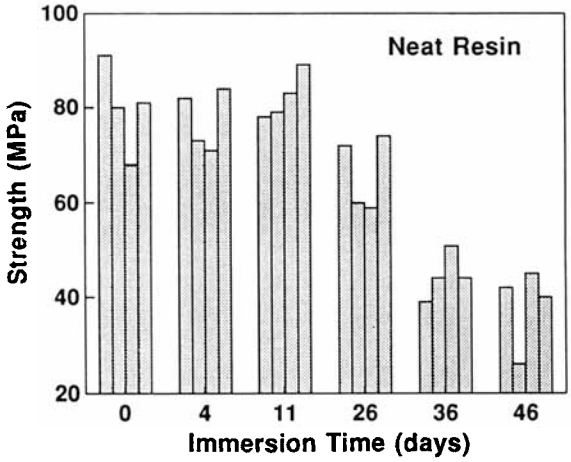

Figure 7 Decrease in tensile strength of neat resin at 23°C after immersion for various times at 100°C.

can be used to calculate the mean stress σ_m (sometimes called *negative pressure*) in the matrix surrounding the silica particle.

In order to simplify the calculation, we consider the filler particles to be spherical, with radius R_1, and enclosed within a spherical shell of resin having an internal radius R_1 and external radius R_2. As the radius of the filler particle remains unchanged throughout the curing reaction, R_1, the internal radius of the resin shell, can be treated as the resultant of two opposing effects: a linear shrinkage of 2.6% due to curing of the resin in the unstressed state, and a linear expansion of 2.6% under internal pressure exerted by the filler particle. This radial expansion from the unstressed state is given the symbol u. For a shell with a shear modulus G and bulk modulus K, under internal pressure p_1 and external pressure p_2, the radial displacement $u(r)$ at a distance r from the center of the particle is given by the following:[7]

$$u(r) = \frac{(p_1R_1^3 - p_2R_2^3)r}{3K(R_2^3 - R_1^3)} + \frac{(p_1 - p_2)R_1^3R_2^3}{4G(R_2^3 - R_1^3)r^2} \quad (4)$$

taking the external pressure p_2 as zero, and rearranging

$$p_1 = \left(\frac{R_2^3 - R_1^3}{R_1^3}\right)\left(\frac{12GKr^2}{4Gr^3 + 3KR_2^3}\right)u. \quad (5)$$

For an element containing 30 vol % filler, $R_2/R_1 = 1.5$. Using this figure, with $G = 1$ GPa and $K = 5$ GPa, Eq. (5) gives the pressure across the interface, where $r = R_1$ and $u/R_1 = 0.026$, as 67.8 MPa.

Table II Fracture Strengths (MPa) at 23°C of Individual Modar Resin (T00F00) Specimens after Immersion for Various Times t_i at 100°C, Followed by Vacuum Drying

Specimen Number	Time t_i (Days)					
	0	4	11	26	36	46
1	91	82	78	72	39	42
2	80	73	79	60	44	26
3	68	71	83	59	51	45
4	81	84	87	74	44	40

The mean stress σ_m in the resin shell is independent of r, and is given by[7]

$$\sigma_m = \frac{p_1 R_1^3 - p_2 R_2^3}{R_1^3 - R_2^3}. \quad (6)$$

With $R_2/R_1 = 1.5$, $p_1 = 67.8$ MPa, as above, and $p_2 = 0$, this gives a mean stress in the resin of 28.5 MPa.

The application of a pressure p to a body of volume V increases its free energy by an amount $\Delta G = \int V\,dp$. For a mixture, there is an increase in the chemical potential of each component. In the present experiments, both filled and unfilled resins are in equilibrium with water under atmospheric pressure, at either 23 or 100°C. Consequently, at a given temperature, the chemical potential of the absorbed water at equilibrium must be the same in all samples. Where the resin is under pressure, this is achieved by reducing the absorbed water concentration, hence the reduction in M_s.

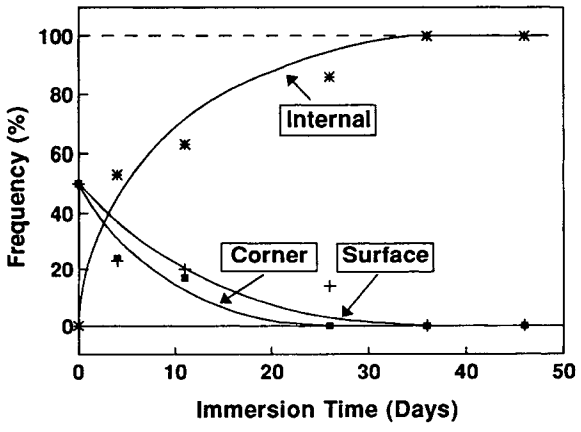

Figure 8 Locations of sites for initiation of fractures in neat resin at 23°C, after immersion for various times at 100°C.

The above treatment is, of course, a simplification. If each imaginary shell of resin is considered to be in contact with its neighbors, shrinkage of the remaining resin regions between the shells will distort them from their original spherical shape, pulling them away from the central filler particle. At high filler concentrations, this effect may be significant.

Fracture

Under conditions of brittle fracture, tensile strength σ_c is related to K_{IC} and initial crack or defect size a_0 through the relationship

$$K_{IC} = Y\sigma_c\sqrt{\pi a_0} \quad (7)$$

When the crack front follows the arc of a circle, the geometrical factor $Y = 2C/\pi$, where $C = 1$, 1.12, and 1.2 for embedded circular disc defects, semicircular surface defects and quarter-circular corner defects, respectively.[8]

Figure 10 shows the relationship between fracture strength σ_c and defect size a_0 in dry Modar 8035, calculated for each of these crack types using Eq. (7), with $K_{IC} = 0.59$ MPa $m^{1/2}$, as given in Table III. For a given defect size, internal flaws give rise to the highest fracture strengths, and corner defects

Table III The Influence of Moisture on Fracture Toughness K_{IC} (MPa $m^{1/2}$) of Modar 8035 Resin and Blends at 23°C[a]

Materials	T00F00	T15F00	T15F46
Normal	0.50	1.47	2.03
Dried	0.59	1.33	1.91
Wet	0.85	1.48	2.05

[a] Measurements were reproducible to ±0.05 MPa $m^{1/2}$.

Note: Specimen thickness is 4 mm for T00F00 and 6 mm for T15F00 and T15F46.

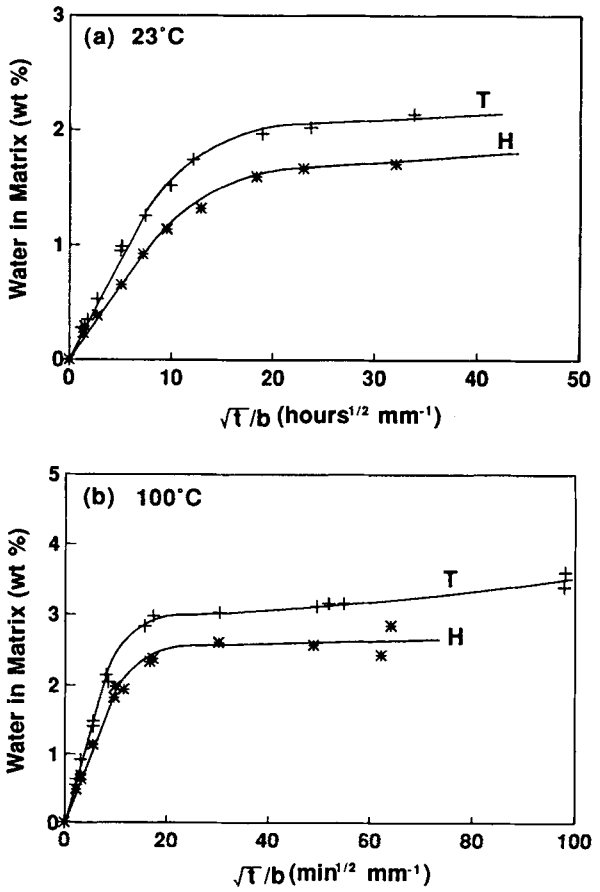

Figure 9 Weight fraction of water absorbed *by the matrix phase* of (T) T15F00-toughened resin; and (H) T15F46 hybrid resin at (a) 23°C and (b) 100°C, as a function of immersion time.

the lowest. That is why all fractures start from either corner or surface defects in Modar samples that have not been exposed to water. The higher Y factor for cracks at corners, where half of them originated in untreated Modar, is offset by the lower probability of finding a large defect very near a corner, as compared with a flat surface.

For neat resin that has been immersed in water at 100°C, the fracture strength σ_c varies with the immersion time, as shown in Table II and Figure 7. On the other hand, calculations based on fracture strength σ_c and defect dimensions show that K_{IC} remained effectively constant. Defect diameters were obtained from microscope observations of fracture surfaces, and are shown in Table IV for individual specimens that failed from an internal flaw. Both minor and major axes $2a$ and $2c$ are listed where they are different. It should be borne in mind that each specimen contains a large number of flaws and defects, and that only the largest, which result in failure, are recorded. Specimen numbers in Table IV correspond to those in Table II. No data are given in Table IV for cracks initiating at corners or surfaces, because of difficulties in defining the dimensions of the initial crack or defect.

The Y factor used in these calculations is[8]

$$Y = \frac{\left(\sin^2\phi + \frac{a^2}{c^2}\cos^2\phi\right)^{1/4}}{\frac{\pi}{8}\left(3 + \frac{a^2}{c^2}\right)} \tag{8}$$

where a, c, and ϕ are defined in Figure 11. The average value of the function $[\sin^2\phi + (a^2/c^2)\cos^2\phi]$ over the range $0 < \phi < 2\pi$, is $(1 + a^2/c^2)/2$. Inserting this value into Eq. (8) we have

$$Y = \frac{\left(\frac{1}{2} + \frac{a^2}{2c^2}\right)^{1/4}}{\frac{\pi}{8}\left(3 + \frac{a^2}{c^2}\right)} \tag{9}$$

Figure 12 compares fracture toughness values of T00F00 specimens, calculated using Eqs. (7) and (9), and data from Tables II and IV. The average value of K_{IC} is 0.59 MPa, in exact agreement with the value obtained from SENB tests (Table III).

The formation of embedded disc cracks around inorganic inclusions clearly indicates that large forces are generated when the inclusions absorb water. The EDAX data suggest that these inclusions

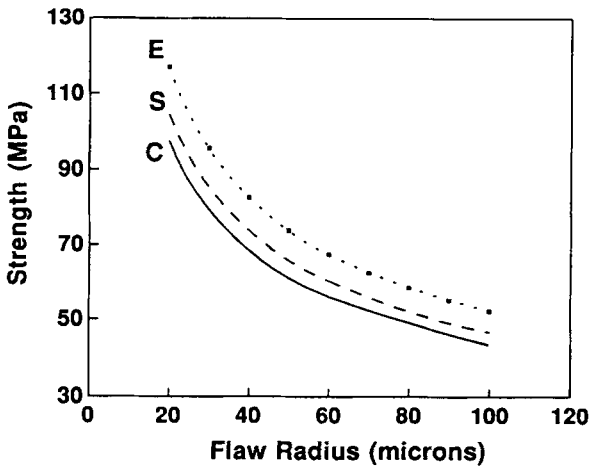

Figure 10 Strength of tensile bar calculated using Eq. (7) for (E) embedded, (S) surface, and (C) corner cracks of circular shape, with K_{IC} = 0.59 MPa $m^{1/2}$.

Table IV Dimensions 2a of the Critical Defect (in Microns) for the Specimens Listed in Table II, Showing Effects of Water Immersion t_i at 100°C (Where $2a \neq 2c$, Both Are Given)

Specimen Number	Time t_i (Days)					
	0[a]	4	11	26	36	46
1	—	75	75/150	100	350/37	450
	—	75	150	100	370	450
2	—	—	—	150	200	800
	—	—	—	150	480	800
3	—	65/125	125	80/300	200	330
	—	125	125	300	320	330
4	—	100	60/110	60/225	450	200/460
	—	100	110	225	450	460

[a] No data are given for $t_i = 0$, because all fractures start from either corner or surface defects.

are dust particles consisting of common minerals such as aluminosilicates. Unlike the products resulting from hydrolysis of polyesters, as described by Lee et al.[1] they are largely insoluble in water, and, therefore, probably do not generate a significant osmotic pressure. On the other hand, solid inorganic compounds are known to undergo large expansions as a result of hydration. Examples are given in Table V, which lists volume increases for four metal salts, calculated from molecular weight and density data on the salts and their hydrates. These figures, together with the evidence from optical microscopy that the inclusions expand substantially in water (see Fig. V), support the view that hydration of inorganic impurities is the major driving force behind the initiation of disc cracks.

Using the relevant value of Y, these results can be used to relate the fracture behavior of Modar 8035 resin to the maximum defect size in the material. From Figure 10, it can be estimated that the critical radius for corner or surface defects in dry, untreated Modar resin varies from 20 to 40 μm: fracture strengths σ_c are in the range 70–90 MPa (Table II). It may be assumed that defects of similar size also exist within the body of the specimen. After the material has been immersed in water, but before disc-like cracks develop, the effective size of these defects appears to increase, especially in the subsurface regions, because there is a sharp rise in the probability that fracture starts from internal defects, as indicated in Figure 8. The radius of the critical internal penny-shaped defect can be estimated from Eq. (7), with the appropriate value of Y, using the K_{IC} value of 0.59 MPa $m^{1/2}$ obtained for dry Modar resin: the σ_c data in Table II on specimens immersed for 4–11 days correspond to defects with maximum radii in the range 43–63 μm.

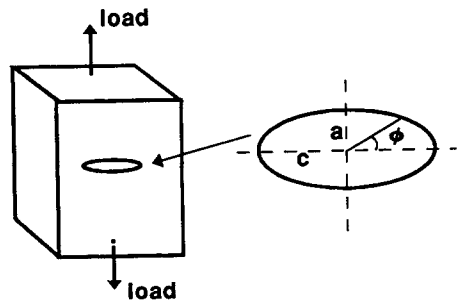

Figure 11 Schematic diagram defining a, c, and ϕ in Eq. (8).

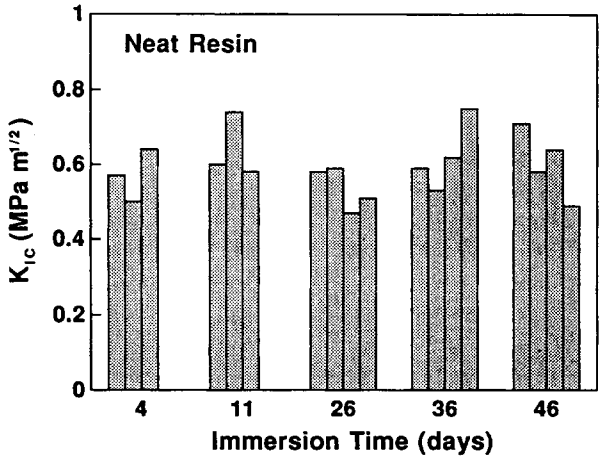

Figure 12 Fracture toughness of neat resin at 23°C, calculated from data given in Figure 7 and Tables II and IV, showing that K_{IC} is independent of immersion time.

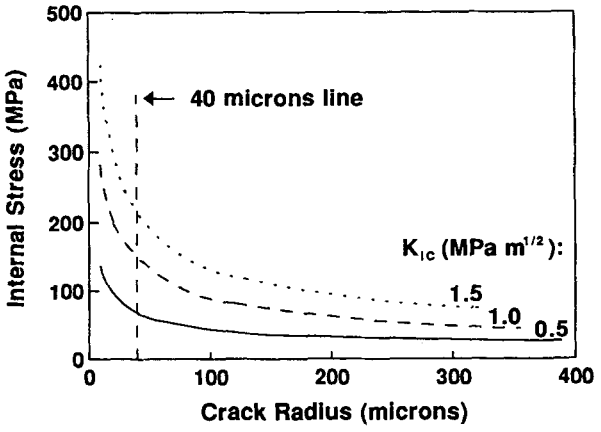

Figure 13 Calculated critical internal stress required for propagation of a disc crack, as a function of K_{IC} and crack radius.

The internal pressures responsible for initiating disc cracks of the type illustrated in Figure 5 can be estimated by treating the filler particle as equivalent to a penny-shaped crack of radius r. The stress intensity factor K_I due to a distributed pressure σ acting internally on the faces of a crack is equal to the K_I obtained when a tensile stress of the same magnitude is applied at infinity.[8] It follows that for the case of embedded circular disc cracks,

$$K_{IC} = \frac{2}{\pi}\sigma_c\sqrt{\pi r}. \qquad (10)$$

If it is assumed that K_{IC} for water-saturated Modar resin is in the range 0.50–1.0 MPa $m^{1/2}$, then the critical internal stress σ_c can be estimated using Eq. (10). For an impurity defect with a radius of $\sim$ 10 μm (Fig. 5), σ_c is 140–260 MPa, depending upon the value assigned to K_{IC}. The relationship between σ_c and defect size is shown in Figure 13 for K_{IC} = 0.5, 1.0, and 1.5 MPa $m^{1/2}$. It is clear that large internal pressures are needed to initiate cracks from the relatively small impurity particles found in Modar resin samples.

There are four obvious ways in which these internal pressures could be generated: osmotic pressure effects of the type proposed by previous authors[1-3]; swelling of the impurities in water; shrinkage during cure; and thermal contraction from the cure temperature. In the Modar samples studied, there was no evidence of soluble inorganic impurities that might generate appreciable osmotic pressures. On the other hand, immersion experiments at 100°C on related urethane–methacrylate resins have shown rapid increases in water uptake after 100–120 days, which are unrelated to visible impurities, and appear to be due to hydrolysis of the resin. This is unlikely to be a significant factor within the time scale of the present experiments. It is clear from the optical micrographs (Fig. 5) that the main cause of disc cracking is that insoluble impurities undergo a substantial degree of swelling. The Modar also swells, but to a lesser extent because the maximum water uptake is only 3.2 wt % (Table I). As discussed earlier, additional internal pressures of about 28 MPa are to be expected around silica filler particles as a result of contraction in the resin during cure and subsequent cooling.

Modar resin will crack when the tangential stress σ_t at the resin–impurity interface reaches a critical value. In order to calculate σ_t, we adopt the spherical shell model used earlier for resin layers adjacent to filler particles, and apply Eq. (4) for the case $R_2 \gg R_1$, and $r = R_1 = R$. The results are[7]

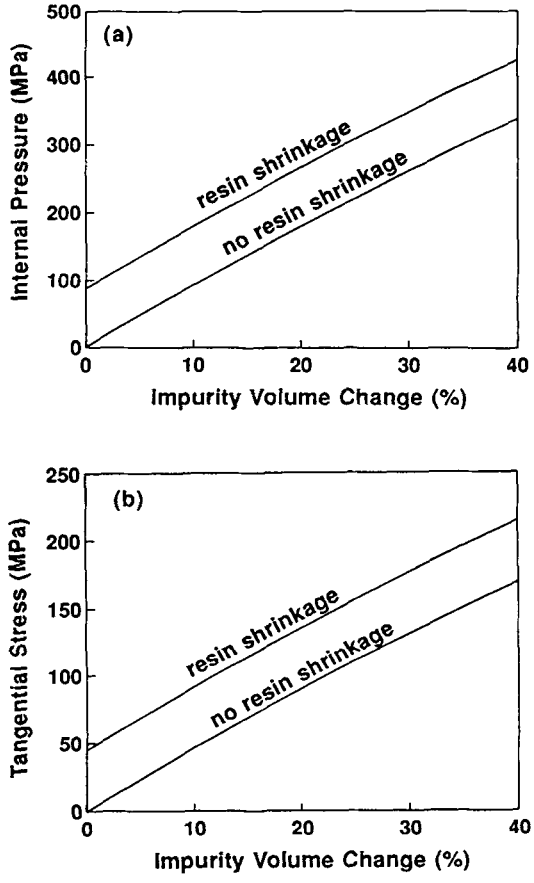

Figure 14 Effect of expansion of spherical solid impurity on (a) internal pressure exerted across interface upon surrounding matrix and (b) tangential stress within the matrix at the interface.

Table V Relative Volume Increase after Formation of Hydrates from Metal Salts

Materials	MWt	ρ (g cm^{-3})	$\Delta V/V$ (%)
$Al_2(SO_4)_3$	342	2.71	—
$Al_2(SO_4)_3 \cdot 18H_2O$	666	1.69	212
Na_2SO_3	158	2.50	—
$Na_2SO_3 \cdot 12H_2O$	474	1.76	326
$Mg(ClO_4)_2$	223	2.21	—
$Mg(ClO_4)_2 \cdot 8H_2O$	331	1.98	66
$MgSO_4$	120	2.66	—
$MgSO_4 \cdot H_2O$	138	2.45	25
$MgSO_4 \cdot 7H_2O$	246	1.68	225

Note. Density data from CRC Handbook.[8]

$$\frac{u}{R} = \frac{p_2}{3K} - \frac{p_1 - p_2}{4G} \tag{11}$$

$$\sigma_t = p_2 - \frac{p_1}{2} \tag{12}$$

where u/R represents the radial strain in the resin, which is related to the corresponding volume strain by

$$\frac{u}{R} = \left(1 + \frac{\Delta V}{V}\right)^{1/3} - 1 \tag{13}$$

Figure 14 shows the results of calculations based on Eq. (11–13), taking $p_2 = 0$, $E = 2$ GPa and $\nu = 0.4$ for water-saturated Modar at 100°C. Internal pressure p_1, and tangential stress σ_t increase almost linearly with the volume strain in the spherical inclusion.

In the present case, an internal pressure of about 86 MPa is generated as a result of 11.3% shrinkage of the resin during cure, followed by 2% volume expansion due to swelling with water. From Eq. (12), the corresponding tangential stress σ_t at the matrix/impurity interface is about 43 MPa. These stresses must be added to those due to expansion of the impurity. The effects of this net shrinkage contribution on p_1 and on σ_t are included in Figure 14. Resin shrinkage might not in itself be sufficient to cause internal cracking, but it becomes very significant in combination with swelling of the impurity particles.

Examples of the expansions that can occur on hydration of metal salts are given in Table V. Volume changes in excess of 300% are not uncommon. It is therefore not surprising that after prolonged exposure to water, an inorganic impurity particle should expand enough not only to crack Modar resin, but also to propagate the crack to several times its own diameter.

Throughout the course of this work, no evidence of disc cracking was found in rubber-modified or hybrid Modar. Fracture strengths remained constant over 46 days immersion in water at 100°C. This is clearly due to the high fracture toughness of the rubber-modified resin. Figure 13 shows that when K_{IC} is greater than 1.5 MPa m$^{1/2}$, critical stresses of over 220 MPa are required in order to develop internal cracks from defects less than 40 μm in diameter.

CONCLUSIONS

This work has shown that diffusion of water through Modar 8035 resin is Fickian, and that Fick's law also applies, at least approximately, to rubber-modified and filled/toughened (hybrid) versions of the resin. For these modified resins, minor deviations from Fickian behavior are seen, especially at 23°C. The presence of a rigid filler reduces the equilibrium water content of the resin matrix, probably as a result of internal pressure generated by shrinkage of the resin during cure. Fracture of neat Modar 8035 resin is defect-dominated. The critical defects are inorganic impurities, probably particulate minerals, and metallic salts, with diameters in the range 40–80 μm. Disc-like cracks are initiated from these impurities when Modar 8035 reaches a critical level of water absorption at 100°C. Contraction of the resin during cure, and swelling of insoluble mineral impurities, combine to set up the internal pressures responsible for these internal cracks.

The authors thank ICI Chemicals & Polymers Ltd for a grant to support X.C.Z.

REFERENCES

1. S. B. Lee, T. J. Rockett, and R. D. Hoffman, *Polymer,* **33,** 2353 (1992).
2. R. F. Fedors, *Polymer,* **21,** 713 (1980).
3. R. F. Fedors, *Polymer,* **21,** 207 (1980).
4. J. G. Williams, *Prog. Rubb. Plast. Technol.* **6,** 174 (1990).
5. J. Crank, *The Mathematics of Diffusion,* Clarendon Press, Oxford, 1957, p. 148.
6. J. Stoddart, Private communication.
7. H. Reismann and P. Pawlik, *Elasticity: Theory and Applications,* Wiley, New York, 1980, p. 152.
8. H. L. Ewalds and R. J. H. Vanhill, *Fracture Mechanics,* Edward Arnold, London, 1986, p. 49.
9. *CRC Handbook of Physics and Chemistry,* 72nd ed, CRC Press, Cleveland, Ohio, 1991–1992.

Received July 12, 1993
Accepted October 17, 1993